Divergence Free Synthetic Eddy Method for LES Inflow Conditions

R. Poletto, A. Revell, T. Craft, N. Jarrin
School of Mechanical, Aerospace & Civil Engineering
The University of Manchester, Manchester M13 9PL, UK

I. Introduction

One of the challenges in performing Large Eddy Simulations (LES) of turbulent flows is the prescription of a suitable velocity field at flow inlets. In most cases these should, ideally, correspond to a suitably realistic unsteady flow field; yet at the same time one also wants them to be reasonably cheap to generate. It is well known that simply imposing random fluctuations on top of a mean velocity field at an inlet will result in a long development length before the flow reaches what might be considered a realistic turbulent state, and so a number of alternative methods have been developed, aimed at providing more realistic representations of inlet turbulence.

Jarrin et al. (2009) developed the Synthetic Eddy Method (SEM) as a quasi-particle based method to generate synthetic turbulence conditions. The method esentially involves the superposition of a (large) number of random eddies, which are convected through a domain of rectangular cross-section, such as that shown in Fig. 1. The resultant, time-dependent, flowfield from a cross-section of this SEM domain is extracted and imposed as inlet conditions for the LES. Using this approach Jarrin et al. (2009) found that LES of a channel flow at $Re_\tau = 395$ required a distance of around 10–12 channel half-widths to become fully-developed. Some further improvements were achieved by Pamiès et al. (2009), by specifically tuning the shape functions associated with the eddy representations for a channel flow. Although they did report a decrease in the required development length, the form adopted would appear to be rather specific to the application.

One of the perceived weaknesses of the above SEM methods is that the imposed inlet flowfield does not satisfy the divergence-free condition. As a consequence of this the LES tends to introduce significant pressure fluctuations close to the inlet (in order to adapt the velocity field to something that does satisfy continuity), and this adds to the required development length. In the present work, we therefore explore a method of extending the SEM approach in order to produce a suitable inlet velocity field that does satisfy continuity.

ruggero.poletto@postgrad.manchester.ac.uk

II. The Divergence Free SEM

In the SEM developed by Jarrin et al. (2006) and Jarrin et al. (2009), the fluctuating velocity field is generated by taking

$$\mathbf{u}'(\mathbf{x}) = \frac{1}{\sqrt{N}} \sum_{k=1}^{N} a_{ij} \varepsilon_j^k f_\sigma(\mathbf{x} - \mathbf{x^k}) \qquad (1)$$

where N is the number of eddies introduced into the SEM domain, $\mathbf{x}_k$ is the location of the centre of the kth eddy, $f_\sigma(\mathbf{x})$ is a suitable shape function, ε_j^k are random numbers and a_{ij} are coefficients. Although this formulation does allow the desired Reynolds stress field to be prescribed (via the a_{ij} coefficients), the velocity field will not, in general, also satisfy continuity.

By employing results from votex dynamics methods (see, for example, Winckelmans and Leonard (1993); Winckelmans et al. (2005)), the above formulation has been adapted, to be written as

$$\mathbf{u}'(\mathbf{x}) = \sqrt{\frac{1}{N}} \sum_{k=1}^{N} \mathbf{K}_\sigma(\frac{\mathbf{x} - \mathbf{x}^k}{\sigma}) \times \{R_L^G(\boldsymbol{\alpha}^k)^L\} \qquad (2)$$

where the vector $\mathbf{K}_\sigma(\mathbf{y})$ is the Biot-Savart kernel, defined as $\mathbf{K}_\sigma(\mathbf{y}) = \frac{q_\sigma(|\mathbf{y}|)}{|\mathbf{y}|^3}\mathbf{y}$ with $q_\sigma(|\mathbf{y}|)$ a suitable shape function. R_L^G is a transformation matrix to rotate the desired Reynolds stress tensor to its principle axes (essentially, therefore, consisting of the three eignevectors of the Reynolds stress tensor). Finally, the vector $(\alpha^k)^L$ is taken as having components $\alpha_i^k = \{C_i \varepsilon_i\}^k$, where the ε_i's are random numbers. If the coefficients C_i are taken as $C_i = \sqrt{\lambda_{max} - 2\lambda_i}$, where the λ's are the eigenvalues of the Reynolds stress tensor, then it can be shown that the form of equation (2) does return the desired Reynolds stress statistics. As a result of the form of equation (2), with certain conditions placed on the form of the shape function q_σ, the resulting velocity field cam also be shown to satisfy the divergence-free condition.

In the present work the shape function has been taken as

$$q_\sigma(y) = \sqrt{\frac{16 V_B}{15\pi\sigma^3}} \left(\sin(\pi y)\right)^2 y \qquad (3)$$

where V_B and σ are prescribed eddy velocity and lengthscales respectively.

III. Results

Initial tests were conducted to confirm that the above DF-SEM method does indeed return a divergence-free velocity field and that, within certain limits, the desired Reynolds stress field could be prescribed. The method was then implemented into the Code-Saturne CFD software to allow further testing, and sample results of the method employed to provide inlet conditions for LES of a plane channel flow at $Re\tau = 395$ are presented below.

Fig. 2 shows the development of the skin friction coefficient, using both the present DF-SEM and the original SEM form of Jarrin et al. (2009). In both cases the input Reynolds stress distribution for the SEM was taken from a RANS calculation of fully developed channel flow using the k-ω SST model. The length-scale σ is prescribed as $\sigma = \max(\min(\frac{k^{\frac{3}{2}}}{\varepsilon}, \kappa\delta), \Delta)$, and the number of eddies, N is sufficiently large to ensure fully developed SEM statistics.

Both schemes show the characteristic initial drop of C_f associated with most LES inlet treatments, followed by a recovery as the LES develops realistic turbulence structures. The original SEM reaches the asymptotic C_f level after around 15 channel halt-heights. The new DF-SEM approach shows a rather different behaviour, with C_f initially appearing to recover more rapidly, but then overshooting, before returning to the asymptotic level slightly earlier than the original scheme. Instantaneous snapshots of inlets produced by the two SEM schemes, and compared to an equivalent fully-developed LES snaphshot, are shown in Fig. 1. These clearly indicate that the structures produced by the DF-SEM approach appear to be much more realistic and comparable to the LES patterns than those generated by the original SEM.

To shed some further light on the performance of the DF-SEM, Fig. 3 shows the development of the turbulence statistics from the LES, in the form of Reynolds stress components at a non-dimensional distance from the wall, y^+, of just under 50. Since the RANS model currently employed to provide the SEM with stress values is a linear eddy-viscosity scheme the normal stresses start from an isotropic state, whilst the shear stress $\overline{uv}$ starts from close to its asymptotic value. There is a fairly rapid development of the stresses, with $\overline{u^2}$ displaying an overshoot before decreasing to its asymptotic level, and corresponding adjustments to the other components (particularly $\overline{v^2}$ and $\overline{uv}$) are also seen. It is believed that the overshoot seen in C_f may well be related to these initial stress adjustments.

The above comments suggest that further improvements might be expected from the use of a better RANS model (eg. a non-linear EVM or stress transport scheme) to provide the Reynolds stress input levels for the DF-SEM, since the consequent development of the stresses should not be as abrupt as seen in Fig. 3. One problem with following this route at present, however, lies in the formulation of the coefficients C_i. For these to be real we clearly need to have $\lambda_{max} - 2\lambda_i$ positive for all the eignenvalues of the Reynolds stress tensor. In the principle axes of the stress tensor this implies that each normal stress should not be greater than $k/2$, where k is the turbulent kinetic energy. To illustrate how restrictive this constraint might be, Fig. 5 shows the possible states of turbulence anisotropy within the Lumley triangle, together with data taken from a turbulent channel flow DNS by Moser et al. (1999), and the limiting line implied by the above constraint. Whilst cleary some level of anisotropy can be accommodated by the present approach, the high levels found in near-wall layers cannot be, without some further modification.

The final paper will give a more detailed derivation and description of the present DF-SEM method, together with validation studies showing its sensitivity to input parameters such as eddy lengthscale, σ, and number of eddies, N. Applications to further test cases will also be presented, together with explorations and possible routes to further develop the formulation in an attempt to circumvent the above limitation on the imposed level of stress anisotropy.

References

Jarrin, N., S. Benhamadouche, D. Laurence, and R. Prosser (2006, August). A synthetic-eddy-method for generating inflow conditions for large-eddy simulations. *International Journal of Heat and Fluid Flow 27*(4), 585–593.

Jarrin, N., R. Prosser, J. Uribe, S. Benhamadouche, and D. Laurence (2009, June). Reconstruction of turbulent fluctuations for hybrid RANS/LES simulations using a Synthetic-Eddy method. *International Journal of Heat and Fluid Flow 30*(3), 435–442.

Moser, R. D., J. Kim, and N. N. Mansour (1999). Direct numerical simulation of turbulent channel flow up to re[sub tau] = 590. *Physics of Fluids 11*(4), 943–945.

Pamiès, M., P.-É. Weiss, E. Garnier, S. Deck, and P. Sagaut (2009). Generation of synthetic turbulent inflow data for large eddy simulation of spatially evolving wall-bounded flows. *Physics of Fluids 21*(4), 045103.

Winckelmans, G., R. Cocle, L. Dufresne, and R. Capart (2005). Vortex methods and their application to trailing wake vortex simulations. *Comptes Rendus Physique 6*(4-5), 467–486. Aircraft trailing vortices.

Winckelmans, G. S. and A. Leonard (1993). Contributions to vortex particle methods for the computation of Three-Dimensional incompressible unsteady flows. *Journal of Computational Physics 109*(2), 247–273.

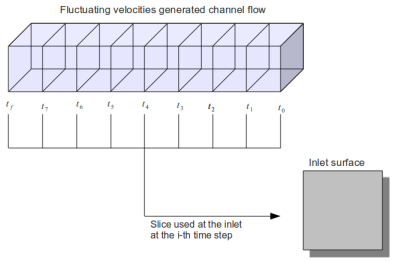

Figure 1. Scheme of the inlet generation for the LES inflow.

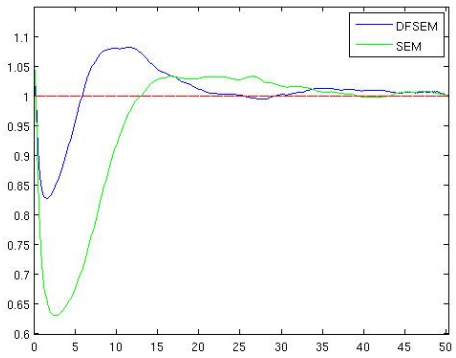

Figure 2. C_f coefficient development along the channel flow.

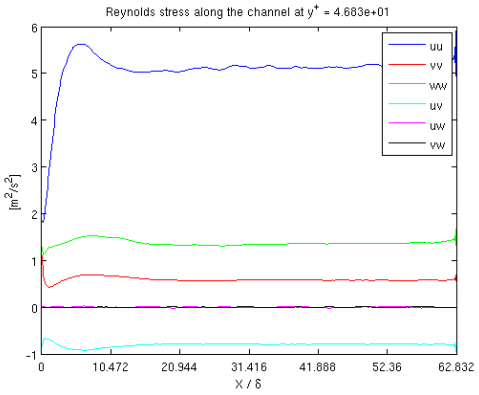

Figure 3. Reynolds stresses development along the Channel flow at $y^+ = 47$.

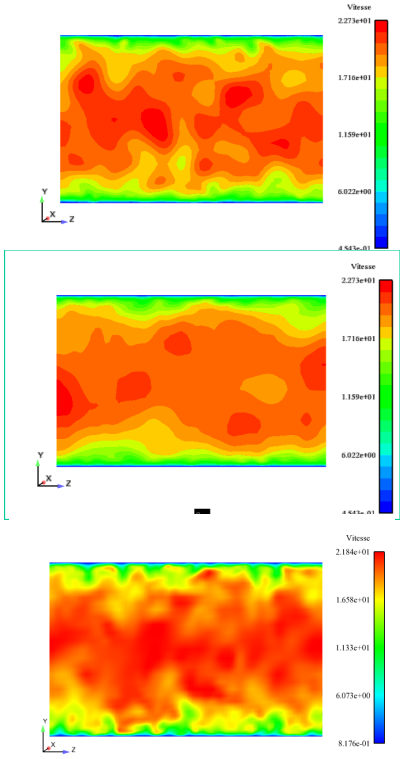

Figure 4. Velocity contour plots of (from top to bottom) DF-SEM, SEM and periodic channel flow

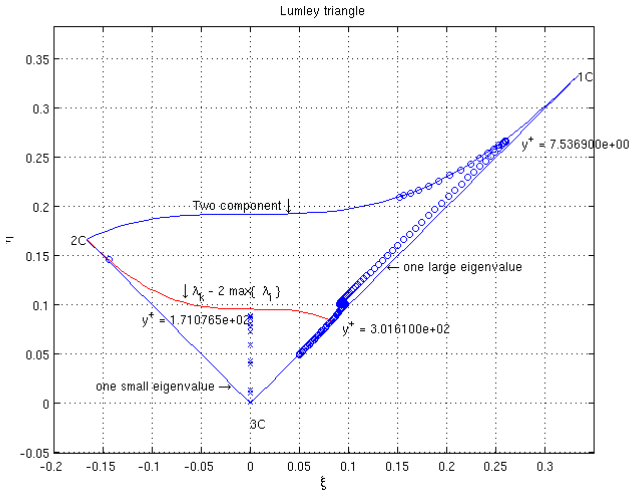

Figure 5. $6\eta^2 = b_{ii}^2$; $6\xi^3 = b_{ii}^3$ and $b_{ij} = \frac{<u_i u_j>}{<u_k u_k>} - \frac{1}{3}\delta_{ij}$. Red line: limit of real solutions for C_i coefficients with the present approach; Symbols used : ◯ channel flow DNS data from Moser et al. (1999), × RANS with $k-\omega$ SST turbulence model.